KeAi
CHINESE ROOTS
GLOBAL IMPACT

Contents lists available at ScienceDirect

Petroleum Science

journal homepage: www.keaipublishing.com/en/journals/petroleum-science



Original Paper

Microscopic accumulation mechanism of helium in shale gas: Insights from molecular simulation



Bing You ^{a,b}, Jian-Fa Chen ^{a,b,*}, Qing-Yong Luo ^{a,b}, Hong Xiao ^{a,b}, Mei-Jun Li ^{a,b,c}, Xiao-Oiang Liu ^{c,**}

- ^a State Key Laboratory of Petroleum Resources and Engineering, China University of Petroleum (Beijing), Beijing, 102249, China
- ^b College of Geosciences, China University of Petroleum (Beijing), Beijing, 102249, China
- ^c Faculty of Petroleum, China University of Petroleum-Beijing at Karamay, Karamay, 834000, Xinjiang, China

ARTICLE INFO

Article history: Received 25 August 2024 Received in revised form 24 March 2025 Accepted 26 June 2025 Available online 3 July 2025

Edited by Xi Zhang and Jie Hao

Keywords: Helium Helium adsorption Shale gas Competitive adsorption Molecular simulation

ABSTRACT

Shale gas in southern China is found to contain economically valuable helium (He), which is inconsistent with conventional perspective that hydrocarbon gases in shale would dilute He to sub-economic levels. The adsorption of gases in the nanopores of organic matter is considered a crucial factor influencing the shale gas composition. The adsorption behaviors of He, methane (CH₄) and their mixtures in kerogen nanopores were performed by the Grand Canonical Monte Carlo simulation. The molecular simulations of pure He reveal that He can be adsorbed in shale and the adsorption capacity of He increases with the burial depth of shale. Before the hydrocarbon generation from kerogen, He has been continually generated in shale, the simulations further demonstrate that pure He can be partially preserved in shale as adsorbed gas phase. The simulations of competitive adsorption between CH4 and He show that the adsorption selectivity of CH₄/He is consistently higher than 1.0 under the simulated conditions. This indicates that the previously adsorbed He will be displaced by CH₄ and subsequently concentrated in hydrocarbon gas as free gas phase during the process of hydrocarbon gas generation from kerogen. After the termination of hydrocarbon gas generation, He continues to be generated in shale and preferentially concentrated in free shale gas. Therefore, the concentration of He in shale gas will gradually increase with the generation time of He. In addition, our simulations indicate that high pressure and deep burial depth can enhance the adsorption of He in kerogen, suggesting that deeply buried organic-rich shale probably retains more adsorbed helium. Molecular simulations of He adsorption provide new insights into the accumulation process of He in shale gas and are of great significance for assessing helium resource potential in shale gas.

© 2025 The Authors. Publishing services by Elsevier B.V. on behalf of KeAi Communications Co. Ltd. This is an open access article under the CC BY-NC-ND license (http://creativecommons.org/licenses/by-nc-nd/4.0/).

1. Introduction

Helium (He) is an exhaustible natural resource, and the industrial He is mainly extracted from natural gas reservoirs, primarily hydrocarbon gas reservoirs (Ballentine and Lollar, 2002; Brown, 2010; Anderson, 2018; Chen et al., 2021). Natural gas with He concentration over 0.1% (fractional volume) is regarded as He-rich natural gas (Ballentine and Lollar, 2002) and He-rich gas reservoirs in

sedimentary basins have commercial extraction value and are also the main targets for He exploration (Nuttall et al., 2012; Liu et al., 2023). He accumulated in sedimentary basins was mainly derived from the decay of radioactive elements, such as uranium and thorium (U and Th) (Oxburgh et al., 1986; Ballentine et al., 2002). Organic matter-rich shales are usually enriched in U (Barnes and Cochran, 1990; Anderson, 2018), but previous studies proposed that shales with high contents of U and Th cannot be effective He source rocks and He-rich gas reservoirs cannot be formed in shales without other He source (Brown, 2010; Wang et al., 2023), because of the intense dilution of He by the hydrocarbon gas that generated from the same shale bed. However, shale gases with He concentrations higher than 0.1% have been discovered in southern China (Luo et al., 2019; Wang et al., 2022) and He in these shale gases is mainly

^{*} Corresponding author.

^{**} Corresponding author.

E-mail addresses: jfchen@cup.edu.cn (J.-F. Chen), xqliu@cupk.edu.cn (X.-Q. Liu). Peer review under the responsibility of China University of Petroleum (Beijing).

generated from the shale with no external source (Wang et al., 2022), which means that He-rich shale gases can exist in sedimentary basins. However, little is known about the helium preservation and accumulation mechanism in shale reservoirs, especially helium overcomes the strong dilution effect of hydrocarbon gases in shale, which seriously restricts the process of helium resource exploration in shale gas.

Shale gas is an important unconventional hydrocarbon gas resource, and mainly stored in the micro and nano pores of shale as free gas, adsorbed gas and dissolved gas, among which dissolved gas is negligible due to the low water content (Curtis, 2002; Jarvie et al., 2007; Li et al., 2022). The adsorbed gas can account for 20%-85% of the total amount of shale gas (Curtis, 2002) and the exploration and development technology of adsorbed gas is gradually improving (Jiang et al., 2014; Wang et al., 2016, 2017). For example, the competitive adsorption of CO₂ and CH₄ in shale gas reservoirs (Huang et al., 2018a; Sui et al., 2020; Zhou et al., 2020; Yu et al., 2021; Bonnaud et al., 2023). In addition, the adsorption and desorption behaviors of shale gas has been extensively investigated (Chen et al., 2018; Huang et al., 2018a; Ma et al., 2020), studies show that clay minerals and organic matter (kerogen) jointly provide the main gas adsorption capacities in shale (Curtis et al., 2011; Hao et al., 2018; Yu et al., 2021). As He and hydrocarbon gas in shale are derived from the same source rock and preserved in the same reservoir, the research of He adsorption mechanism in shale is necessary for revealing the He accumulation process in shale gas.

Molecular simulation as a useful computer modelling technology is widely applied in unconventional natural gas exploration (Liu et al., 2016, 2020; Huang et al., 2018a; Li et al., 2021; Yu et al., 2021). He with single molecular structure and small kinetic diameter has prominent advantages in molecular simulation, the adsorption and diffusion characteristics of He in quartz have been investigated using molecular simulation (Liu et al., 2024; Song et al., 2024; You et al., 2024). Liu et al. (2024) and Song et al. (2024) investigated the diffusion characteristics of He in mineral nanopores and demonstrated that the diffusion ability of He decreases when mixed with other gases, which favors the preservation of He. Additionally, You et al. (2024) revealed that He can be adsorbed in quartz surface under high pressure conditions and adsorbed He can be replaced by CH₄ based on the molecular simulation of isotherm adsorption of He, which promotes the enrichment of He in hydrocarbon gases. Molecular simulation on He adsorption behaviors can provide deeper understanding of microscopic mechanism of He migration and accumulation.

This study focuses on the effect of temperature, pressure and burial depth on the adsorption mechanisms of pure He, CH₄ and CH₄-He binary mixtures by molecular simulation. This study reveals the microscopic mechanism of He accumulation, which has important guiding significance for the exploration of He in shale gas and provides an important theoretical basis for future research.

2. Computational details

2.1. Molecular model

Previous studies show that most of adsorbed shale gas was found in organic pores, and kerogen is a major component of sedimentary organic matter in shale and rich in nanopores (Ross and Bustin, 2009; Zhang et al., 2012; Huang et al., 2018a; Yu et al., 2021). At present, the construction technology of kerogen models is mature and kerogen molecular models have been established in many studies (Collell et al., 2014; Bousige et al., 2016; Gao et al., 2017). Thus, in our simulation, type I kerogen at late oil window was choose as adsorbent, and the kerogen model unit with a formula of $C_{208}H_{168}N_4O_{10}$ that developed by Gao et al. (2017) was used. Subsequently, 24 optimized kerogen molecules were selfassembled into a large cubic box by performing Amorphous Cell Module in Materials Studio (MS). In order to avoid overlapping between molecules, the initial density of kerogen cell was set to 0.30 g/cm^3 with a formula of $C_{4992}H_{4032}N_{96}O_{240}$. According to the previously reported methods (Liu et al., 2020), a series of molecular dynamic simulations were carried out by using Forcite code in MS. As shown in Fig. 1, when the system reaches dynamic equilibrium, the true density of kerogen cell was determined to be 1.14 g/cm³, which is good agreement with the reported density of $1.14 \pm 0.02 \text{ g/}$ cm³ for kerogen IIIA (Huang et al., 2018b).

2.2. Grand Canonical Monte Carlo (GCMC) simulation

GCMC simulations were performed by using Sorption code to simulate the adsorption mechanisms of He-rich shale gas. The Condensed-phase Optimized Molecular Potentials for Atomistic Simulation Studies (COMPASS) force field (Sun et al., 1998) was taken into account in the whole simulation processes. In our simulations, non-bond energies were determined by using both electrostatic and Van der Waals interactions. The Ewald summation method was applied to calculate the long-range Coulomb interaction with an accuracy of 10^{-5} kcal/mol. The atom-based summation

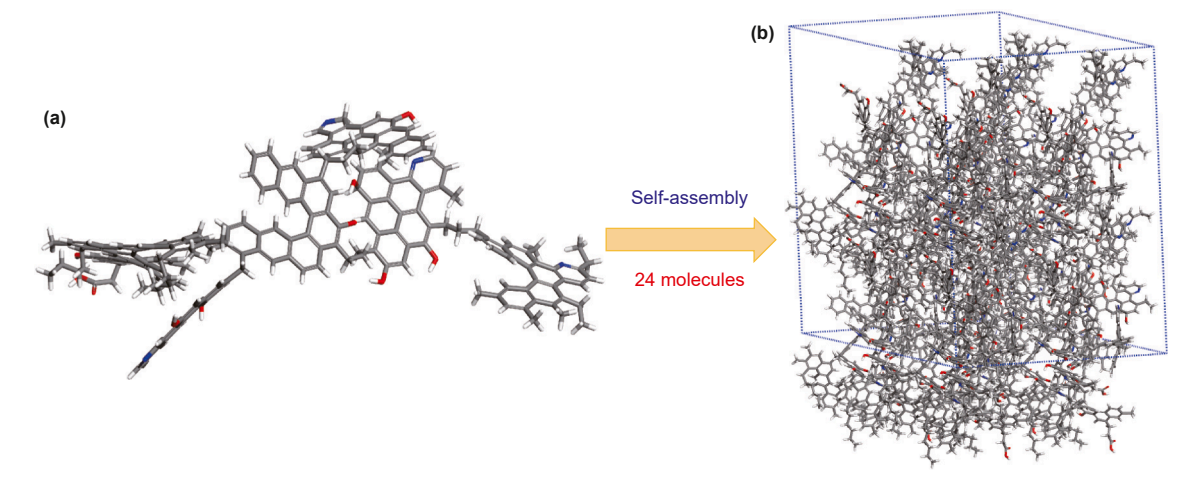


Fig. 1. Kerogen at late oil window (a) and kerogen cell (b).

method was adopted to determine the short-range Van der Waals interaction with a cutoff length of 1.85 nm and a bond width of 0.1 nm. Both adsorption isotherm and fixed-pressure simulations comprised a total of 11×10^7 Monte Carlo steps, of which 1×10^7 were system equilibrium steps and 10×10^7 were statistical average steps. The adsorption capacity (Γ , cm³/g) was defined as follows:

$$\Gamma = \frac{NV_{\rm m}}{M} \times 1000 \tag{1}$$

where N is the number of adsorbed molecules, M is the relative molecular mass of the adsorbent, and $V_{\rm m}$ is the molar volume ($V_{\rm m}=22.414~{\rm L/mol}$ under standard conditions).

The adsorption isotherms were evaluated by the Langmuir model,

$$\Gamma = \Gamma_{\text{max}} \frac{\kappa p}{1 + \kappa p} \tag{2}$$

where $\Gamma_{\rm max}$ (cm³/g) is the largest gas adsorption capacity, p (MPa) is pressure and κ (MPa⁻¹) is the Langmuir coefficient.

The adsorption heat (Q) was calculated using the Clausius-Clapeyron equation (Pan et al., 1998):

$$Q = RT^2 \left(\frac{\partial \ln p}{\partial T} \right)_{\Gamma} \tag{3}$$

where R is the ideal constant (8.314 J mol⁻¹ K⁻¹), T is the temperature (K), and p is the pressure (Pa).

To evaluate the competitive adsorption and adsorption priority of mixed gas, adsorption selectivity ($S_{\text{CH}_a/\text{He}}$) is defined as:

$$S_{\text{CH}_4/\text{He}} = \frac{x_{\text{CH}_4}/x_{\text{He}}}{y_{\text{CH}_4}/y_{\text{He}}} \tag{4}$$

where x_{CH_4} and x_{He} are the mole fractions of CH₄ and He in the adsorbed phase, respectively; y_{CH_4} and y_{He} are the mole fractions of CH₄ and He in the bulk phase, respectively.

2.3. Simulation conditions

2.3.1. Gas components

First, the adsorption behaviors of pure CH_4 and He were simulated in the kerogen nanopores to investigate their adsorption mechanisms and compare their adsorption capacities both in the

molecular simulation of isotherm adsorption and adsorption at temperature and pressure coupled conditions. Second, the competitive adsorption behavior of binary mixtures of CH₄-He in the kerogen nanopores was simulated. Actually, He mole fraction in natural gas reservoirs is very low, the number of helium molecules in the model is determined by the He mole fraction, and the adsorption characteristics of He will be indistinct when a few He molecules present in the model. In order to better exhibit the competitive adsorption mechanisms of He and CH₄, 50% mole fraction of He was set in the molecular simulation of isotherm adsorption to determine the effects of temperature and pressure, respectively. In addition, 0.5%, 5% and 50% mole fraction of He was set in adsorption simulation at temperature and pressure coupled conditions to better reveal the adsorption characteristics of He and CH₄ under geological conditions.

2.3.2. Temperature and pressure settings

In this study, the isothermal adsorption behaviors of CH₄, He and CH₄-He (1:1) in the kerogen nanopores were simulated at different temperatures of 298.15, 323.15, 373.15, 423.15 and 473.15 K under the pressure range of 0–50 MPa. In order to investigate the effect of burial depth on the gas adsorption behaviors in the kerogen nanopores, the geological depth in the range of 200–5000 m was considered at corresponding temperature and pressure conditions. In the simulation, the surface temperature was set at 20 °C and the geothermal and pressure gradients were set at 19 °C/km (Yuan et al., 2006) and 10 MPa/km, respectively.

3. Results and discussion

3.1. Langmuir isotherm adsorption of pure gases

Pure CH_4 and He isothermal adsorptions in kerogen nanopores were simulated at different temperatures by GCMC simulations. Adsorption isotherms of pure CH_4 and He under pressure of 0–50 MPa were plotted in Fig. 2. The isotherms are fitted by the Langmuir model, and the Langmuir model has good fitting accuracy for CH_4 and He adsorption isotherms is higher than 0.95 and 0.99, respectively (R^2 is the coefficient of determination). The adsorption capacity of CH_4 and He both increase with increasing pressure, and decrease with increasing temperature (Fig. 2). The CH_4 adsorption isotherms exhibit a rapid increase, reaching adsorption equilibrium at

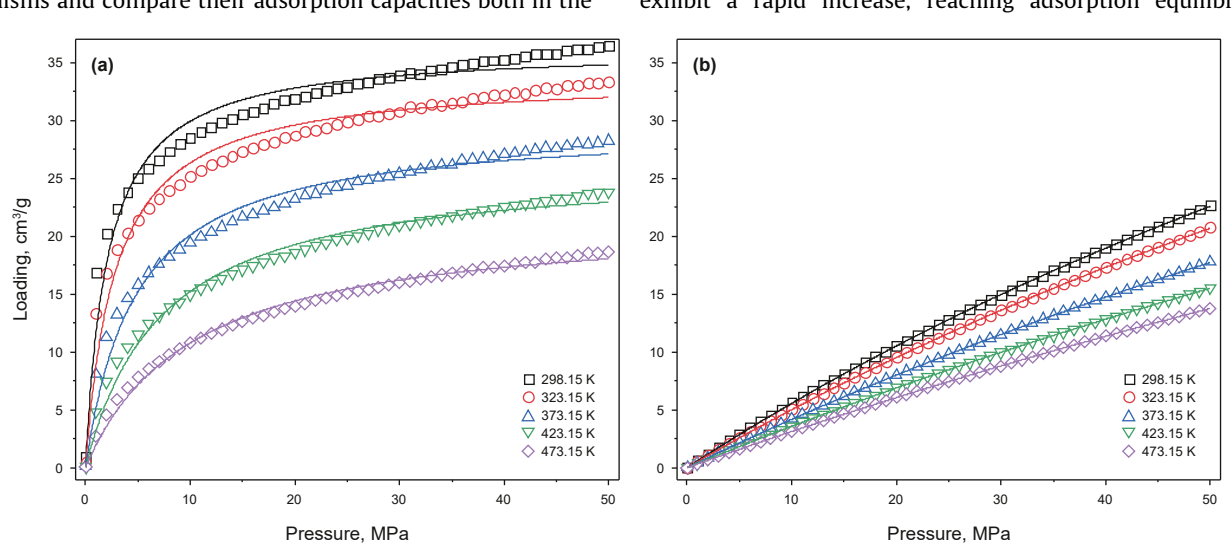


Fig. 2. Adsorption isotherms and Langmuir fittings of pure CH₄ (a) and He (b) in kerogen nanopores at different temperatures.

relatively low pressure (~15 MPa) (Fig. 2(a)), which is consistent with previous studies (Huang et al., 2018a; Wang et al., 2018). In contrast, He adsorption isotherms do not reach adsorption equilibrium even at 50 MPa (Fig. 2(b)). He is a monatomic molecule with a kinetic diameter of 0.26 nm, while CH₄ molecule has a tetrahedral structure with a kinetic diameter of 0.38 nm (Grynia and Griffin, 2016), which determines that the stronger compressibility of He compared to CH₄ in the same pore volume and the smaller size He can be more effectively packed in the pores to reduce the local pressure at high loadings (Sha and Faller, 2016), resulting in that as the pressure increases, the adsorption capacity of He will gradually increases and He is more difficult to reach adsorption equilibrium than CH₄.

Though the adsorption capacity of CH₄ is higher than that of He (Fig. 2) under the highest simulation pressure of 50 MPa, the linear correlations between temperature and the maximum adsorption capacity of pure gases show that the maximum adsorption capacity of He is significantly higher than that of CH₄ at the same temperature (Fig. 3). This may be resulted from that the adsorption capacity of CH₄ will not increase with increasing pressure after the CH₄ adsorption isotherm rapidly reaches adsorption equilibrium at relatively low pressure, whereas the He adsorption isotherm will slowly reaches adsorption equilibrium at very high pressure. The maximum adsorption capacity of CH₄ and He both decreases with increasing temperature, but that of CH₄ decreases more significantly than that of He when temperature increases from 298.15 to 473.15 K (Fig. 3). This indicates that the maximum adsorption capacity of He in kerogen nanopores is less affected by temperature, but mainly controlled by pressure. Before the adsorption isotherm of He reach adsorption equilibrium, the adsorption capacity of He will continually increase with increasing pressure.

3.2. Effect of geological depth on pure gas adsorption

Actually, temperature and pressure are inseparable under geological conditions, increasing simultaneously as the geological burial depth increases, which means that temperature and pressure jointly influence gas adsorption in shale during the process of deep burial and tectonic uplift. In this study, the adsorption of pure CH₄ and He in kerogen nanopores with different burial depth from 200 to 5000 m was simulated to investigate their adsorption behaviors under geological conditions and better discuss geological

phenomena. Fig. 4(a) shows the adsorption behavior of pure He, revealing a gradual increase in adsorption capacity with increasing burial depth, whereas the adsorption capacity of CH_4 increases rapidly as the depth increases from 200 to 1500 m and then reach the adsorption equilibrium at the depth approximately 1800 m at the simulated temperature and pressure conditions.

The isosteric heat values of He and CH₄ range from 0.83 to 1.00 and 5.30 to 5.37, respectively. Obviously, the isosteric heat of CH₄ adsorption is higher than that of He (Fig. 4(b) and (c)), indicating a stronger interaction between CH₄ and kerogen compared with He and kerogen. This implies that CH₄ is preferentially adsorbed in kerogen nanopores when coexisting with He in shale. Moreover, the isosteric heat value of CH₄ gradually decreases with burial depth, while that of He shows an opposite increasing trend. Combined with the simulation results of isothermal adsorption of pure gases, these different trends indicate that pressure plays a dominant role in the adsorption of He in kerogen, whereas temperature has a stronger effect on the adsorption of CH₄ in kerogen.

He and CH₄ in shale gas reservoirs have completely different generation characteristics and independent generation process, He is slowly and continually generated after the formation of U and Th containing minerals (Brown, 2010), while CH₄ is only generated in a fixed evolution stage of organic matters (Wang et al., 2022). Therefore, He has been generated in shale before the generation of CH₄. Though some He that generated before CH₄ would dissolve in pore fluids (Torgersen and Clarke, 1985) or diffuse out of shale (Wang et al., 2022), based on the pure He adsorption behaviors in kerogen nanopores (Fig. 2), some He can also be preserved in shale as adsorbed gas. In addition, the adsorption capacity of He increases with increasing burial depth of shale before the generation of CH₄ (Fig. 4(a)), which indicates that the continuous deep burial of shale is beneficial for the adsorption and preservation of He.

3.3. Langmuir isotherm adsorption of mixed gas

Previous studies have shown that temperature and pressure are both effective factors on the competitive adsorption behaviors of CH₄ and CO₂ of shale gas (Huang et al., 2018b; Wang et al., 2018; Zhou et al., 2018). However, the effects of temperature and pressure on the adsorption of CH₄-He binary mixtures in kerogen have not been reported. In this study, the competitive adsorption behaviors of binary mixture of CH₄-He (1:1) in kerogen nanopores were simulated at different temperatures by GCMC simulations.

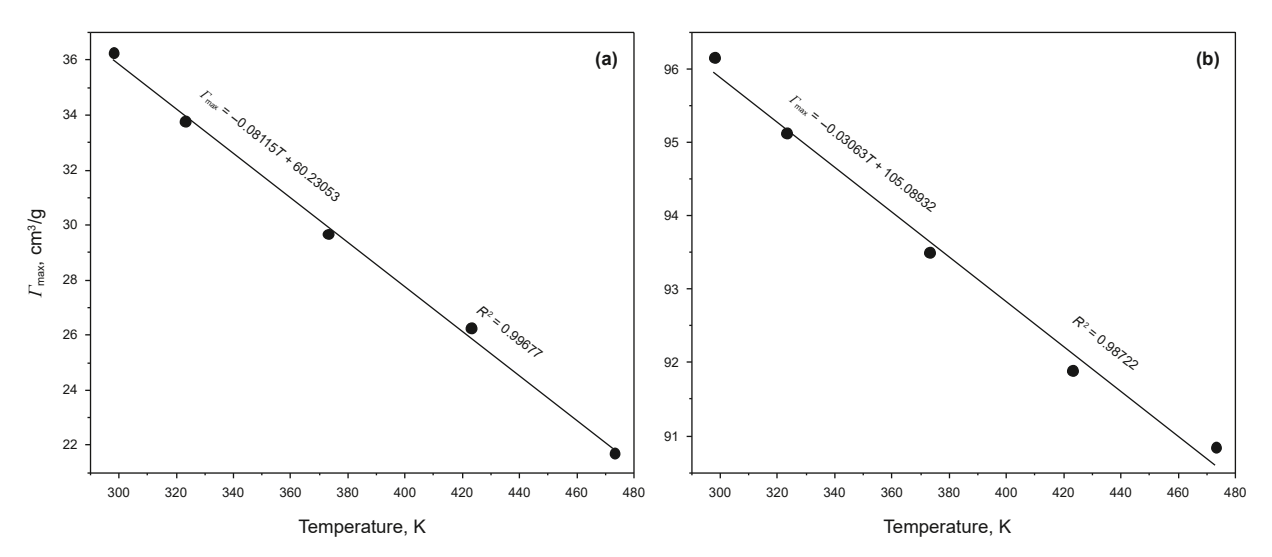


Fig. 3. The relationships between temperature and the maximum adsorption capacity of pure CH₄ (a) and He (b).

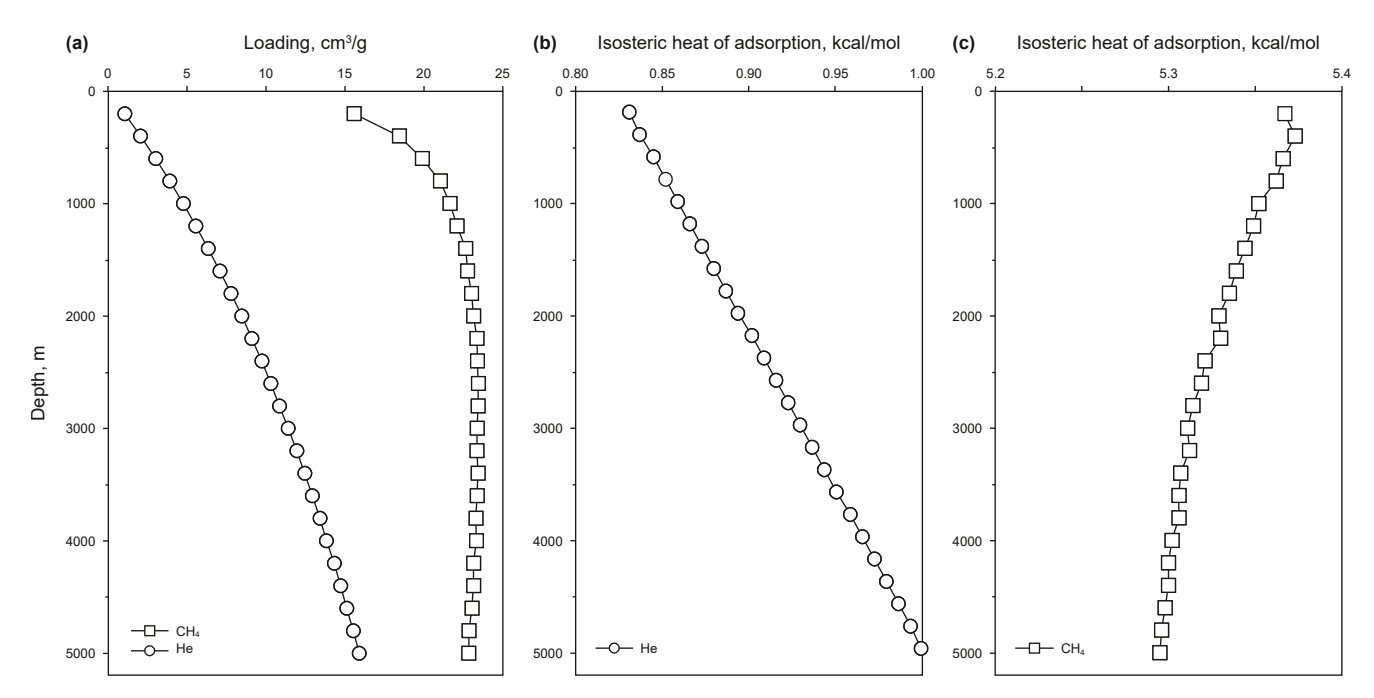


Fig. 4. The pure CH₄ and He adsorption (a) and corresponding isosteric heat of He (b) and CH₄ (c) in kerogen nanopores at different burial depth.

The adsorption isotherms of mixed gas under pressures ranging from 0 to 50 MPa were plotted in Fig. 5(a). The isotherms are fitted by the Langmuir model, and the Langmuir model has good fitting accuracy for helium adsorption isotherms (R^2 is in the range of 0.95-0.99, R^2 is the coefficient of determination). The variation trend of mixed gas adsorption isotherm closely resembles that of pure CH₄ (Fig. 1(a) and 4(a)), which indicates that the mixed gas adsorption in kerogen nanopores is mainly controlled by CH₄. The He adsorption capacity in mixed gas is significantly lower compared to pure He adsorption capacity (Fig. 2(b) and 5(b)), attributed to the competitive adsorption of CH₄ and He. To better understand the competitive adsorption mechanism between CH₄ and He, the adsorption selectivity (CH₄/He) is utilized. From Fig. 6, the adsorption selectivity consistently remains above 1.0 under the simulated conditions. This means that CH₄ exhibits a higher adsorption capacity than He in kerogen nanopores and further

indicates that the previously adsorbed He would be displaced by CH₄. Moreover, the value of CH₄/He adsorption selectivity rapidly decreases with increasing pressure in the range of 0–10 MPa, and tends to achieve equilibrium when the pressure exceeds 40 MPa (Fig. 6). Thus, the lower the pressure, the stronger the competitive adsorption of CH₄, the larger the amount of displaced He.

Due to the generation of hydrocarbon gas in shale, the previously adsorbed He in kerogen nanopores will be displaced by CH₄ and then concentrated in the hydrocarbon gas as free gas phase. In addition, based on the high value of CH₄/He adsorption selectivity in these shales (Fig. 6), adsorbed He will be substantially displaced by CH₄ in relatively low pressured shales, and then He will accumulate in the shale gases. The displacement of adsorbed He is favorable for the accumulation of He in free shale gases, but the amount of displaced He is trivial compared to the yield of shale gases. As the generation process of CH₄ is concentrated and rapid

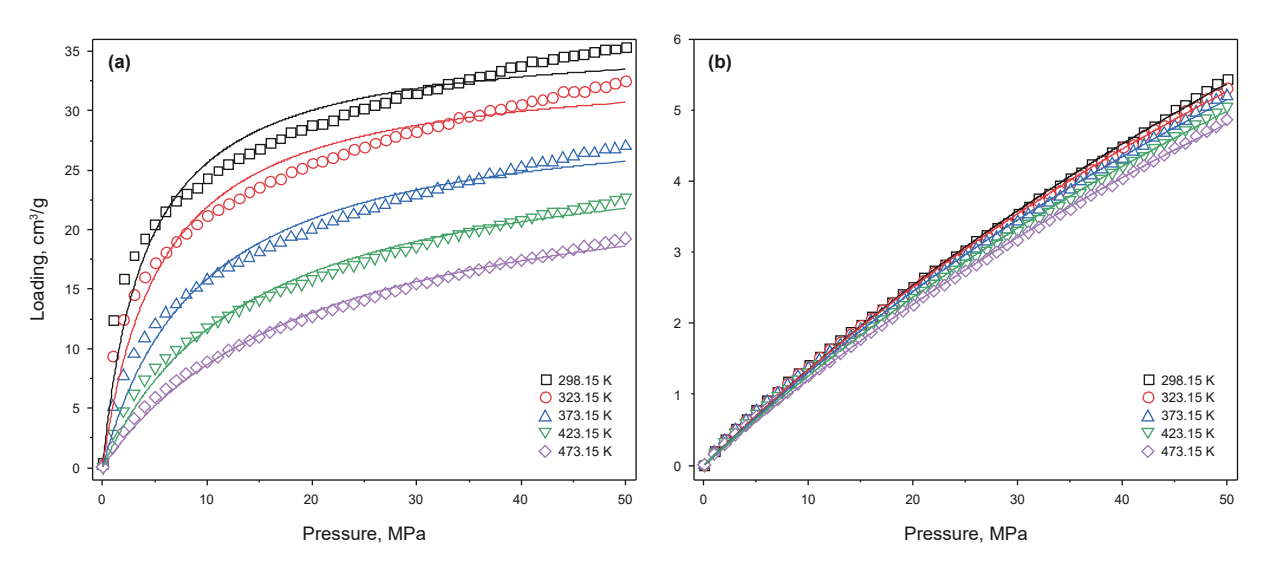


Fig. 5. Adsorption isotherms of mixed gases (a) and He in the mixed gases (b) in kerogen nanopores at different temperatures.

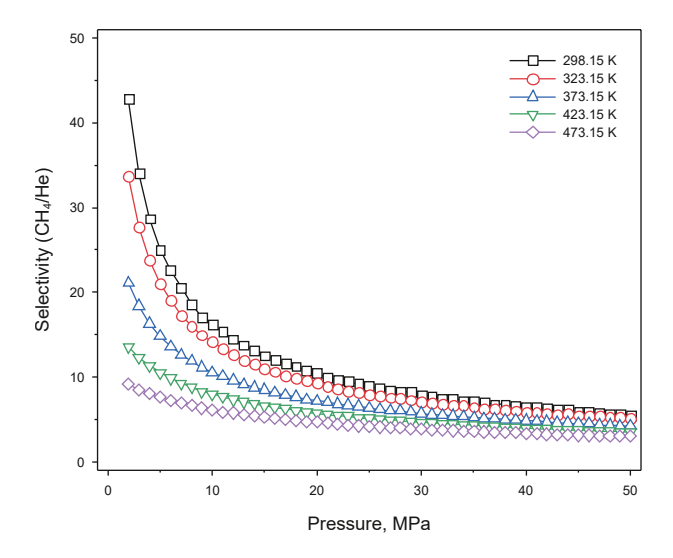


Fig. 6. The adsorption selectivity of CH₄/He at different temperatures.

compared with He and the yield of CH₄ is much higher than He, He in free gas phase will be intensively diluted by CH₄ to subeconomic levels (Brown, 2010). Furthermore, although the amount of displaced He may increase with the increasing content of CH₄ in shale, the relative concentration of He in the free gas phase still decreases with the rapid increase of shale gas yields, which finally contribute to the low concentration of He in shale gases. However, regardless of the concentration of He in shale gas, the competitive adsorption mechanism between CH₄ and He remains a plausible mechanism for He accumulation in shale gas.

3.4. Effect of geological depth on mixed gases adsorption

Geological depth is a key influencing factor for the competitive adsorption behaviors of mixed gases, such as CH_4-CO_2 , CH_4-N_2 and CO_2-N_2 (Liu et al., 2020). Thus, in order to investigate the competitive adsorption behaviors of CH_4 -He binary mixtures under geological conditions and reveal the He accumulation process in shale gases, the burial depth that ranges from 200 to 5000 m has been taken into account in this study. The competitive adsorption behaviors of CH_4 -He binary mixtures with different He mole fractions (0.5%, 5% and 50%) in kerogen nanopores at different burial depth were simulated.

With an increase in burial depth beyond 200 m, the adsorption capacity of He gradually increases with increasing depth (Fig. 7 (b)), the adsorption capacity of CH₄ and mixed gas initially experiences a sharp rise, followed by a gradual increase or a slight decrease (Fig. 7(a) and (c)), whereas the adsorption selectivity of CH₄/He displays an initial sharp decline, followed by a gradual decrease (Fig. 7(d)). As Fig. 7 shown, the adsorption capacity of He decrease with the decrease of He mole fraction, while the adsorption capacities of CH₄ and mixed gases show increase characteristics, in addition, the He mole fraction almost have no effect on the variation trends of adsorption capacity and adsorption selectivity with geological burial depth. The values of the adsorption selectivity of CH₄/He indicates that though the competitive adsorption between CH₄ and He weakens with increasing burial depth, CH₄ will replace adsorbed He under simulated conditions, regardless of the helium mole fraction in the mixed gas.

The isosteric heat of adsorption of CH_4 and He in the mixed gas show quite different variations (Fig. 8). As the increase of burial depth, the isosteric heat of adsorption of CH_4 slightly decreases (Fig. 8(b)), but that of He slightly increases (Fig. 8(a)). This indicates a weakening interaction between CH_4 and kerogen with increasing burial depth, while the interaction between He and kerogen is enhanced. The variations in isosteric heat of adsorption for CH_4 and He at geological conditions indirectly reflect the variation of CH_4/He adsorption selectivity.

In conclusion, high pressure and deep burial depth can enhance the adsorption of He in kerogen (Fig. 4(a) and 8(a)), indicating that deeply buried organic-rich shale probably retains more adsorbed helium.

3.5. Accumulation mechanism of helium in shale gas

Generally, the generation of hydrocarbon gas will be terminated driven by the tectonic uplift (He et al., 2017). During the process of uplift, the temperature and pressure gradually decreases corresponding to the decrease of burial depth, resulting in the desorption of previously adsorbed He and the larger the distance of tectonic uplift, the higher the amount of desorbed He (Fig. 7(a)). In addition, the adsorption selectivity of CH_4/He shows an increasing trend as the burial depth decreases, which indicates that the adsorbed He is partially displaced by CH_4 , and the adsorption selectivity of CH_4/He becomes higher with larger tectonic uplift distances (Fig. 7(d)). And a higher amount of He is displaced and released during the uplift stage. Consequently, this desorbed and displaced He that released in the uplift stage will concentrate in shale gases as free phase, which reveals a mechanism for He accumulation in shale gases.

The generation of He cannot be affected by tectonic uplift, He that generated in the uplift stage will preferentially dissolve into the shale gas instead of adsorbing in shale. Because the large amounts of free CH₄ in the pore space of shale and the strong competitive adsorption of CH₄ both negatively affecting the adsorption of He in shale. Thus, though the He concentration in the free shale gases is very low (Byrne et al., 2018; Wang et al., 2022), the He concentration will gradually increase as the generation time of He increases. The He concentrations in the lower Paleozoic shale gases of southern China are different in different areas (Fig. 9), the average He concentration in the Pengshui, Jiaoshiba and Changning gas fields are 0.083%, 0.038% and 0.021%, respectively (Wang et al., 2022). This is probably caused by the different timings of tectonic uplift in different areas, in detail, the timing of uplift in the Pengshui, Jiaoshiba and Changning areas are 130 (Li et al., 2016), 90 (Li et al., 2016), 65 Ma (Liu et al., 2021), respectively. In addition, the distance of tectonic uplift in the Pengshui area is largest, followed by the Jiaoshiba area and then Changning area (Fig. 9) (Wang et al., 2022), which result in the high amount of desorbed and displaced He in Pengshui shale gas, medium in Jiaoshiba shale gas and low in Changning shale gas. Thus, the relatively long generation time of He after the tectonic uplift and the relatively large amount of desorbed and displaced He in Pengshui area, may jointly contribute to the relatively high He concentration in Pengshui shale gas. Though the tectonic uplift may result in the partial loss of natural gases in shale, the accumulation of helium in shale gas reservoirs at late period cannot be affected. The uplift distance and timing of tectonic uplift are two factors that affect the He concentration in shale gas, but it should be noted that it is still uncertain whether they are the decisive factors.

Consequently, based on the evolutionary process of kerogen, the He accumulation process in shale gas can be divided into

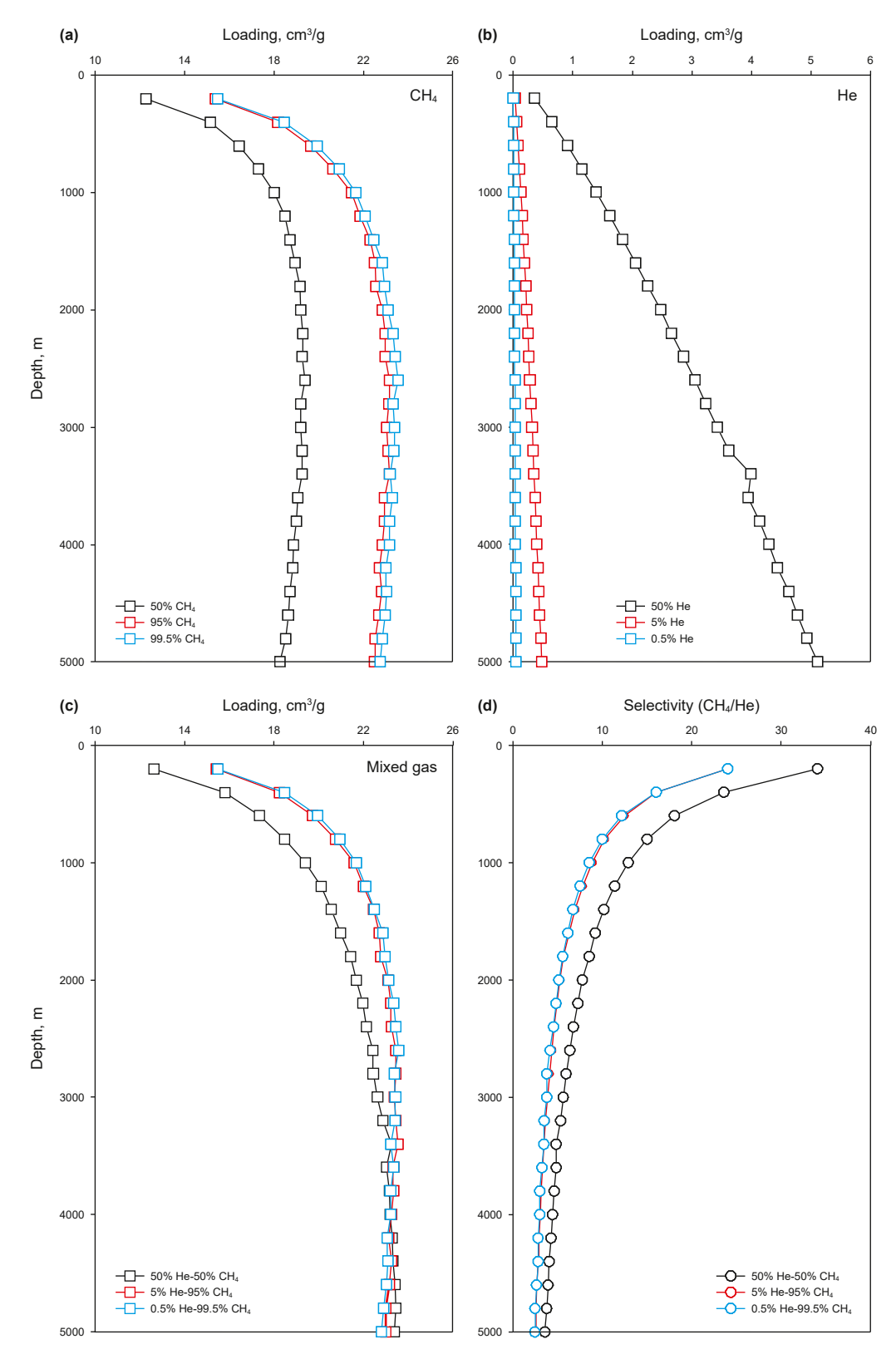


Fig. 7. Adsorption amount of CH₄ (a), He (b), mixed gas (c) and the CH₄-He selectivity (d) at different burial depth.

three stages: (1) hydrocarbon has not been generated from the kerogen. He continually generates, and is partially adsorbed and preserved in shale (Fig. 10(a)), the adsorption amount of He increases with increasing burial depth based on the pure He

adsorption simulation under geological conditions (Fig. 4(a)). (2) Hydrocarbon gas is generated from kerogen. Because of the stronger adsorption capacity of CH_4 than that of He, the previously adsorbed He is displaced by CH_4 and then concentrated in

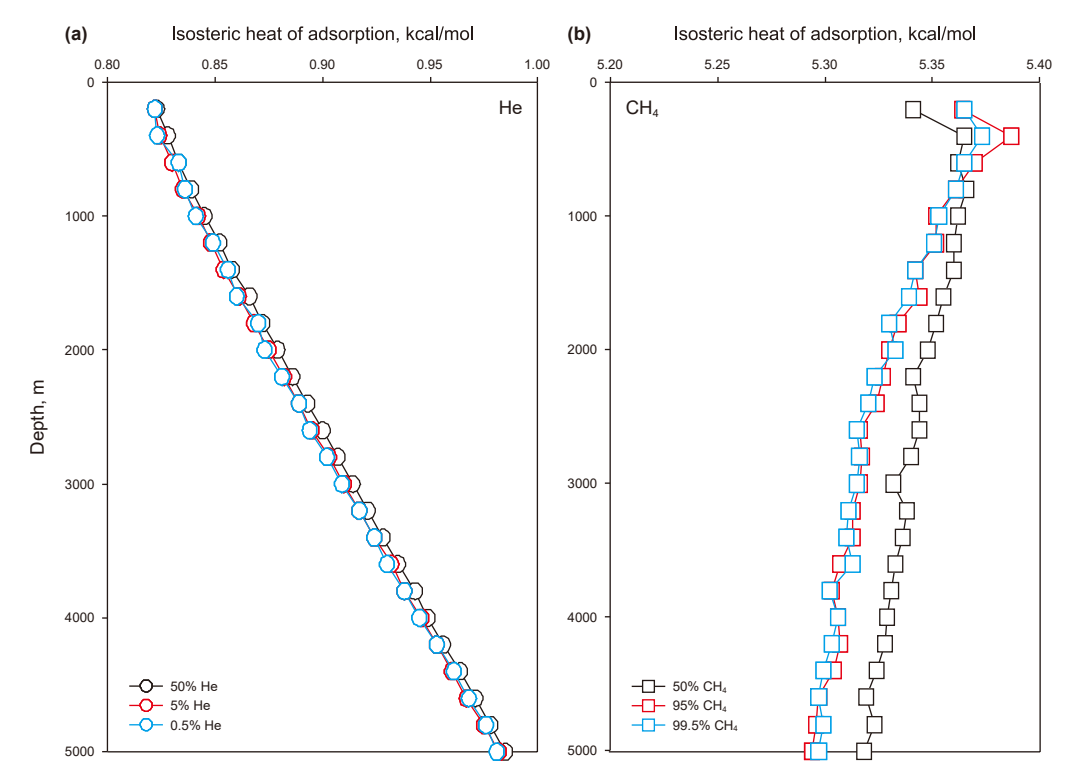


Fig. 8. The isosteric heat of adsorption of He (a) and CH₄ (b) in the mixed gas at different burial depth.

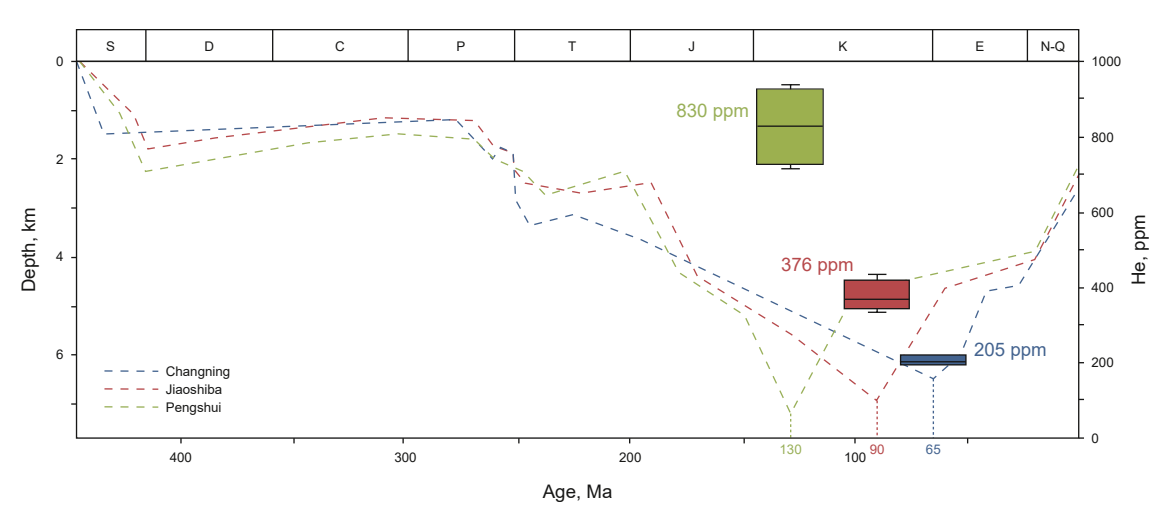
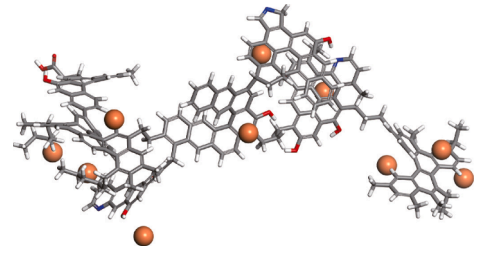


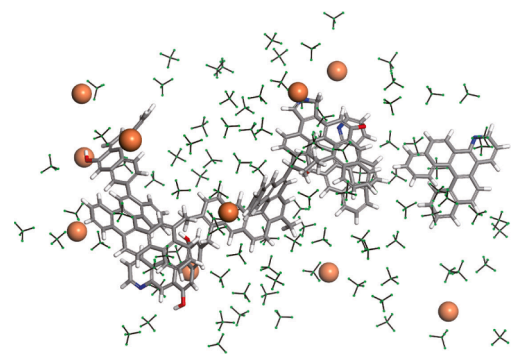
Fig. 9. The burial history of the lower Paleozoic shale and the helium concentrations of Changning, Jiaoshiba and Pengshui areas in Southern China (modified from Wang et al., 2022).

hydrocarbon gas as free phase, simultaneously, He is intensively diluted by the large yields of hydrocarbon gas (Fig. 10(b)). (3) The generation of hydrocarbon gas is terminated. He is still generated

in shale and preferentially dissolve in shale gas, and the concentration of He is gradually increase with increasing generation time of He (Fig. 10(c)).



(a) Before hydrocarbon generation from kerogen



(b) During hydrocarbon gas generation from kerogen

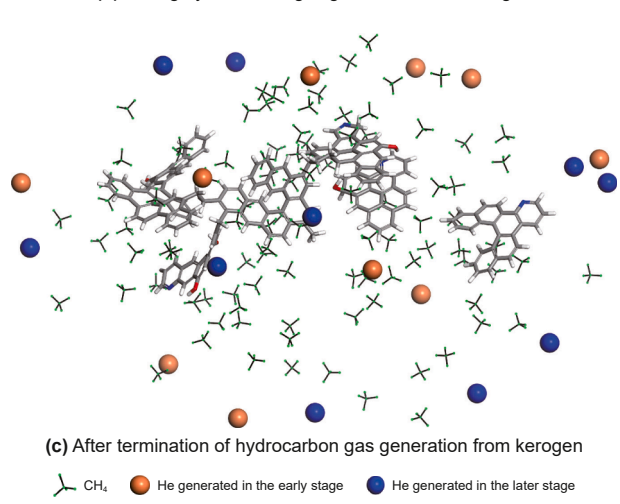


Fig. 10. The adsorption characteristics of helium in kerogen model.

4. Conclusions

Pure He can be adsorbed and preserved in kerogen nanopores based on the molecular simulations of pure He adsorption. The adsorption capacity of He is mainly controlled by pressure, and gradually increases with burial depth. The adsorption capacity of $\mathrm{CH_4}$ is stronger than that of He in kerogen nanopores based on the molecular simulations of competitive adsorption of $\mathrm{CH_4}$ and He. Moreover, the competitive adsorption of $\mathrm{CH_4}$ weakens with increasing burial depth.

The He accumulation process in shale gas can be divided into three stages. In the first stage, the deep burial process of shale can promote the adsorption and preservation of He before the hydrocarbon generation from kerogen. In the second stage, the previously adsorbed He in kerogen nanopores will be displaced by CH₄ during the generation of hydrocarbon gas from kerogen. Then the displaced He will dissolve in hydrocarbon gases as free gas phase, which is a probable accumulation mechanism of He in shale gas. In the third stage, He that generated after the termination of

hydrocarbon gas generation by tectonic uplift will preferentially dissolve in shale gas, then the He concentration in shale gas will gradually increase even reach the economic level. The uplift distance determines the displaced amount of adsorbed He, and the timing of tectonic uplift influences the generation amount of He after the termination of hydrocarbon gas generation. These two factors jointly affect the He concentration in free shale gas.

CRediT authorship contribution statement

Bing You: Writing – original draft, Data curation, Conceptualization. **Jian-Fa Chen:** Funding acquisition, Conceptualization. **Qing-Yong Luo:** Supervision, Investigation, Data curation. **Hong Xiao:** Writing – original draft, Investigation, Formal analysis. **MeiJun Li:** Supervision, Methodology, Investigation. **Xiao-Qiang Liu:** Validation, Software, Methodology, Funding acquisition, Data curation.

Declaration of competing interest

The authors declare that they have no known competing financial interests or personal relationships that could have appeared to influence the work reported in this paper.

Acknowledgments

This study was supported by the National Key Research and Development Program of China (Grant No. 2021YFA0719000), the Science Foundation of China University of Petroleum, Beijing (No. 2462025XKBH007) and the Research Foundation of China University of Petroleum-Beijing at Karamay (No. XQZX20240019).

References

Anderson, S.T., 2018. Economics, helium, and the U.S. federal helium reserve: summary and outlook. Nat. Resour. Res. 27, 455–477. https://doi.org/10.1007/s11053-017-9359-y.

Barnes, C.E., Cochran, J.K., 1990. Uranium removal in oceanic sediments and the oceanic U balance. Earth Planet. Sci. Left. 97, 94–101. https://doi.org/10.1016/ 0012-821X(90)90101-3.

Ballentine, C.J., Sherwood Lollar, B., 2002. Regional groundwater focusing of nitrogen and noble gases into the Hugoton-Panhandle giant gas field, USA. Geochem. Cosmochim. Acta 66 (14), 2483–2497. https://doi.org/10.1016/S0016-7037(02)00850-5.

Ballentine, C.J., Burgess, R., Marty, B., 2002. Tracing fluid origin, transport and interaction in the crust. Rev. Mineral. Geochem. 47, 539–614. https://doi.org/ 10.1515/9781501509056-015.

Bonnaud, P.A., Oulebsir, F., Galliero, G., et al., 2023. Modeling competitive adsorption and diffusion of CH₄/CO₂ mixtures confined in mature type-II kerogen: insights from molecular dynamics simulations. Fuel 352, 129020. https://doi.org/10.1016/j.fuel.2023.129020.

Bousige, C., Ghimbeu, C.M., Vix-Guterl, C., et al., 2016. Realistic molecular model of kerogen's nanostructure. Nat. Mater. 15, 576–582. https://doi.org/10.1038/nmat4541.

Byrne, D.J., Barry, P.H., Lawson, M., et al., 2018. Determining gas expulsion vs retention during hydrocarbon generation in the Eagle Ford Shale using noble gases. Geochem. Cosmochim. Acta 241, 240–254. https://doi.org/10.1016/j.gca.2018.08.042.

Brown, A.A., 2010. Formation of high helium gases: A guide for explorationists. AAPG Search and Discovery. http://www.searchanddiscovery.com/documents/ 2010/80115brown/ndx_brown.pdf.html.

Chen, J., Liu, K., Dong, Q., et al., 2021. Research status of helium resources in natural gas and prospects of helium resources in China. Nat. Gas Geosci. 32 (10), 1436–1449. https://doi.org/10.11764/j.issn.1672-1926.2021.08.006 (in Chinese).

Chen, M., Kang, Y., Zhang, T., et al., 2018. Methane adsorption behavior on shale matrix in-situ pressure and temperature conditions: measurement and modeling. Fuel 228, 39–49. https://doi.org/10.1016/j.fuel.2018.04.145.

Collell, J., Ungere, P., Galliero, G., et al., 2014. Molecular simulation of bulk organic matter in Type II Shales in the middle of the oil formation window. Energy Fuels 28, 7457–7466. https://doi.org/10.1021/ef5021632.

Curtis, J.B., 2002. Fractured shale-gas systems. AAPG Bull. 86, 1921–1938. https://doi.org/10.1306/61EEDDBE-173E-11D7-8645000102C1865D.

Curtis, M.E., Ambrose, R.J., Sondergeld, C.H., et al., 2011. Investigation of the relationship between organic porosity and thermal maturity in the Marcellus

Shale. In: North Am. Unconv. Gas Conf. Exhib. Society of Petroleum Engineers, The Woodlands, Texas, USA. https://doi.org/10.2118/144370-MS.

- Grynia, E., Griffin, P.J., 2016. Helium in natural gas occurrence and production. Gas Liquids Eng. 1 (2), 162–215. https://doi.org/10.7569/jnge.2016.692506.
- Gao, Y., Zou, Y., Liang, T., et al., 2017. Jump in the structure of Type I kerogen revealed from pyrolysis and ¹³C DP MAS NMR. Org. Geochem. 112, 105–118. https://doi.org/10.1016/j.orggeochem.2017.07.004.
- Hao, Y., Yuan, L., Li, P., et al., 2018. Molecular simulations of methane adsorption behavior in illite nanopores considering basal and edge surfaces. Energy Fuels 32, 4783–4796. https://doi.org/10.1021/acs.energyfuels.8b00070.
- He, Z., Hu, Z., Nie, H., et al., 2017. Characterization of shale gas enrichment in the Wufeng Formation-Longmaxi Formation in the Sichuan Basin of China and evaluation of its geological construction-transformation evolution sequence. J. Nat. Gas Geosci. 2, 1–10. https://doi.org/10.1016/j.jnggs.2017.03.002.
- Huang, L., Ning, Z., Wang, Q., et al., 2018a. Molecular simulation of adsorption behaviors of methane, carbon dioxide and their mixtures on kerogen: effect of kerogen maturity and moisture content. Fuel 211, 159–172. https://doi.org/ 10.1016/j.fuel.2017.09.060.
- Huang, L., Ning, Z., Wang, Q., et al., 2018b. Effect of organic type and moisture on CO₂/CH₄ competitive adsorption in kerogen with implications for CO₂ sequestration and enhanced CH₄ recovery. Appl. Energy 210, 28–43. https://doi.org/10.1016/j.apenergy.2017.10.122.
- Jarvie, D.M., Hill, R.J., Ruble, T.E., et al., 2007. Unconventional shale-gas systems: the Mississippian Barnett Shale of north-central Texas as one model for thermogenic shale-gas assessment. AAPG Bull. 91 (4), 475–499. https://doi.org/10.1306/12190606068.
- Jiang, J., Shao, Y., Younis, R.M., 2014. Development of a multi-continuum multi-component model for enhanced gas recovery and CO₂ storage in fractured shale gas reservoirs. In: SPE Improved Oil Recovery Symposium. Tulsa, Oklahoma, USA. https://doi.org/10.2118/169114-MS.
- Li, M., Liu, X., Han, Q., et al., 2021. Progress of molecular simulation application research in petroleum geochemistry. Oil Gas Geol. 42 (4), 919–930. https://doi.org/10.11743/ogg20210413 (in Chinese).
- Li, M., Pang, X., Xiong, L., et al., 2022. The main controlling factors on shale gas occurrence characteristics in deep and high-over mature shales: a case study of Silurian Longmaxi Formation in the Sichuan Basin, Southern China. Energy Rep. 8, 6901–6913. https://doi.org/10.1016/j.egyr.2022.05.037.
- Li, S., Yuan, Y., Sun, W., et al., 2016. Formation and destruction mechanism as well as major controlling factors of the Silurian shale gas overpressure in the Sichuan Basin, China. J. Nat. Gas Geosci. 1, 287–294. https://doi.org/10.1016/j.jnggs.2016.09.002.
- Liu, K., Chen, J., Fu, R., et al., 2023. Distribution characteristics and controlling factors of helium-rich gas reservoirs. Gas Sci. Eng. 110, 204885. https://doi.org/ 10.1016/j.jgsce.2023.204885.
- Liu, X., He, X., Qiu, N., et al., 2016. Molecular simulation of CH₄, CO₂, H₂O and N₂ molecules adsorption on heterogeneous surface models of coal. Appl. Surf. Sci. 389, 894–905. https://doi.org/10.1016/j.apsusc.2016.08.021.
- Liu, X., Li, M., Zhang, C., et al., 2020. Mechanistic insight into the optimal recovery efficiency of CBM in subbituminous coal through molecular simulation. Fuel 266, 117137. https://doi.org/10.1016/j.fuel.2020.117137.
- Liu, X., You, B., Chen, J., et al., 2024. The competitive diffusion mechanism of helium and methanein quartz nanopore by molecular simulation. J. Yangtze Univ. (Nat. Sci. Ed.) 21, 86–94. https://doi.org/10.16772/j.cnki.1673-1409.2024.03.009 (in Chinese).
- Liu, W., Wu, J., Jiang, H., et al., 2021. Cenozoic exhumation and shale-gas enrichment of the Wufeng-Longmaxi Formation in the southern Sichuan Basin, Western China. Mar. Petrol. Geol. 125, 104865. https://doi.org/10.1016/j.marpetgeo.2020.104865.
- Luo, S., Chen, X., Liu, A., et al., 2019. Geochemical features and genesis of shale gas from the lower Cambrian Shuijingtuo Formation shale in Yichang block, middle Yangtze region. Oil Gas Geol. 40, 999–1010. https://doi.org/10.11743/ ogg/20190505 (in Chinese).
- Ma, Y., Zhong, N., Yao, L., et al., 2020. Shale gas desorption behavior and carbon isotopic variations of gases from canister desorption of two sets of gas shales

- in South China. Mar. Petrol. Geol. 113, 104127. https://doi.org/10.1016/j.marpetgeo.2019.104127.
- Nuttall, W.J., Clarke, R.H., Glowacki, B.A., 2012. Resources: Stop squandering helium. Nature 485 (7400), 573–575. https://doi.org/10.1038/485573a.
- Oxburgh, E.R., O'Nions, R.K., Hill, R.I., 1986. Helium isotopes in sedimentary basins. Nature 324, 632–635. https://doi.org/10.1038/324632a0.
- Pan, H., Ritter, J.A., Balbuena, P.B., 1998. Examination of the approximations used in determining the isosteric heat of adsorption from the Clausius—Clapeyron equation. Langmuir 14 (21), 6323–6327. https://doi.org/10.1021/la9803373.
- Ross, D.J.K., Bustin, R., 2009. The importance of shale composition and pore structure upon gas storage potential of shale gas reservoirs. Mar. Petrol. Geol. 26, 916–927. https://doi.org/10.1016/j.marpetgeo.2008.06.004.
- Song, D., Guan, P., Zhang, C., et al., 2024. Molecular dynamics simulations of helium transport through inorganic mineral nanopores. SCI. China Earth Sci. 68, 237–252. https://doi.org/10.1007/s11430-024-1441-y.
- Sui, H., Zhang, F., Wang, Z., et al., 2020. Effect of kerogen maturity, water content for carbon dioxide, methane, and their mixture adsorption and diffusion in kerogen: a computational investigation. Langmuir 36, 9756–9769. https://doi.org/10.1021/acs.langmuir.0c01191.
- Sha, H., Faller, R., 2016. Molecular simulation of adsorption and separation of pure noble gases and noble gas mixtures on single wall carbon nanotubes. Comput. Mater. Sci. 114, 160–166. https://doi.org/10.1016/j.commatsci.2015.12.031.
- Sun, H., Ren, P., Fried, J., 1998. The COMPASS force field: parameterization and validation for phosphazenes. Comput. Theor. Polym. Sci. 8, 229–246. https:// doi.org/10.1016/S1089-3156(98)00042-7.
- Torgesen, T., Clarke, W.B., 1985. Helium accumulation in groundwater, I: an evaluation of sources and the continental flux of crustal 4He in the great Artesian Basin, Australia. Geochem. Cosmochim. Acta 49, 1211–1218. https://doi.org/10.1016/0016-7037(85)90011-0.
- Wang, J., Dong, M., Yang, Z., et al., 2017. Investigation of methane desorption and its effect on the gas production process from shale: Experimental and mathematical study. Energy Fuels 31, 205–216. https://doi.org/10.1021/acs.energyfuels.6b02033.
- Wang, T., Tian, S., Li, G., et al., 2018. Selective adsorption of supercritical carbon dioxide and methane binary mixture in shale kerogen nanopores. J. Nat. Gas Sci. Eng. 50, 181–188. https://doi.org/10.1016/j.jngse.2017.12.002.
- Wang, X., Zhai, Z., Jin, X., et al., 2016. Molecular simulation of CO₂/CH₄ competitive adsorption in organic matter pores in shale under certain geological conditions. Petrol. Explor. Dev. 43, 841–848. https://doi.org/10.1016/S1876-3804(16) 30100-8.
- Wang, X., Liu, W., Li, X., et al., 2022. Application of noble gas geochemistry to the quantitative study of the accumulation and expulsion of lower Paleozoic shale gas in Southern China. Appl. Geochem. 146, 105446. https://doi.org/10.1016/j. apgeochem.2022.105446.
- Wang, X., Liu, Q., Liu, W., et al., 2023. Helium accumulation in natural gas systems in Chinese sedimentary basins. Mar. Petrol. Geol. 150, 106155. https://doi.org/ 10.1016/j.marpetgeo.2023.106155.
- You, B., Chen, J., Liu, X., et al., 2024. Adsorption behavior of helium in quartz slit by molecular simulation. Sci. Rep. 14, 18529. https://doi.org/10.1038/s41598-024-69298-3.
- Yu, X., Li, J., Chen, Z., et al., 2021. Determination of CH₄, C₂H₆ and CO₂ adsorption in shale kerogens coupling sorption-induced swelling. Chem. Eng. J. 410, 127690. https://doi.org/10.1016/j.cej.2020.127690.
- Yuan, Y., Ma, Y., Hu, S., et al., 2006. Present-Day geothermal characteristics in South China. Chin. J. Geophys. 49, 1118–1126. https://doi.org/10.3321/j.issn:0001-5733.2006.04.025 (in Chinese).
- Zhang, T., Ellis, G.S., Ruppel, S.C., et al., 2012. Effect of organic-matter type and thermal maturity on methane adsorption in shale-gas systems. Org. Geochem. 47, 120–131. https://doi.org/10.1016/j.orggeochem.2012.03.012.
- Zhou, J., Jin, Z., Luo, K., 2020. The role of brine in gas adsorption and dissolution in kerogen nanopores for enhanced gas recovery and CO₂ sequestration. Chem. Eng. J. 399, 125704. https://doi.org/10.1016/j.cej.2020.125704.
- Zhou, W., Zhang, Z., Wang, H., et al., 2018. Molecular insights into competitive adsorption of CO₂/CH₄ mixture in shale nanopores. RSC Adv. 8, 33939. https:// doi.org/10.1039/C8RA07486K.